Identification of a Major Epitope Recognized by PLA2R Autoantibodies in Primary Membranous Nephropathy

Maryline Fresquet,* Thomas A. Jowitt,* Jennet Gummadova,† Richard Collins,* Ronan O'Cualain,* Edward A. McKenzie,† Rachel Lennon,*‡§ and Paul E. Brenchley§‖

*Wellcome Trust Centre for Cell-Matrix Research, Manchester, United Kingdom; †Manchester Institute of Biotechnology, Manchester, United Kingdom; ‡Institute of Human Development, Manchester, United Kingdom; §Central Manchester University Hospitals NHS Foundation Trust, Manchester Academic Health Science Centre, Manchester, United Kingdom; and ‖Institute of Cardiovascular Sciences, University of Manchester, Manchester, United Kingdom

ABSTRACT

Phospholipase A_2 receptor 1 (PLA2R) is a target autoantigen in 70% of patients with idiopathic membranous nephropathy. We describe the location of a major epitope in the N-terminal cysteine-rich ricin domain of PLA2R that is recognized by 90% of human anti-PLA2R autoantibodies. The epitope was sensitive to reduction and SDS denaturation in the isolated ricin domain and the larger fragment containing the ricin, fibronectin type II, first and second C-type lectin domains (CTLD). However, in nondenaturing conditions the epitope was protected against reduction in larger fragments, including the full-length extracellular region of PLA2R. To determine the composition of the epitope, we isolated immunoreactive tryptic fragments by Western blotting and analyzed them by mass spectrometry. The identified peptides were tested as inhibitors of autoantibody binding to PLA2R by surface plasmon resonance. Two peptides from the ricin domain showed strong inhibition, with a longer sequence covering both peptides (31-mer) producing 85% inhibition of autoantibody binding to PLA2R. Anti-PLA2R antibody directly bound this 31-mer peptide under nondenaturing conditions and binding was sensitive to reduction. Analysis of PLA2R and the PLA2R-anti-PLA2R complex using electron microscopy and homology-based representations allowed us to generate a structural model of this major epitope and its antibody binding site, which is independent of pH-induced conformational change in PLA2R. Identification of this major PLA2R epitope will enable further therapeutic advances for patients with idiopathic membranous nephropathy, including antibody inhibition therapy and immunoadsorption of circulating autoantibodies.

J Am Soc Nephrol 26: 302–313, 2015. doi: 10.1681/ASN.2014050502

Idiopathic membranous nephropathy (IMN) is a rare form of GN affecting 10–12 cases per million population.[1] The important discovery in 2009 that circulating antibodies to phospholipase A_2 receptor 1 (PLA2R) are present in 70% of patients with IMN identified the autoimmune nature of this pathologic abnormality.[2] Genetic evidence of the involvement of PLA2R in IMN came from the genome-wide association study identifying *PLA2R* and *DQA1* as genes accountable for the genetic susceptibility to IMN.[3] Clinical confirmation that anti-PLA2R antibodies are relevant in MN is evident from studies showing an association between high levels of anti-PLA2R and active disease,[4,5] poor clinical outcome at 5 years,[5,6] and less chance of spontaneous remission.[7] Failure to render patients anti-PLA2R seronegative by immunosuppression therapy is associated with high risk of relapse.[8]

Received May 21, 2014. Accepted August 26, 2014.

P.E.B. and R.L. contributed equally to this work.

Published online ahead of print. Publication date available at www.jasn.org.

Correspondence: Professor Paul Brenchley, Renal Research Labs, Manchester Royal Infirmary, Oxford Road, Manchester M13 9WL, United Kingdom, or Dr. Rachel Lennon, Wellcome Trust Centre for Cell-Matrix Research, Michael Smith Building, University of Manchester, Manchester M13 9PT, United Kingdom. Email: paul.brenchley@manchester.ac.uk or Rachel.Lennon@manchester.ac.uk

In other autoimmune kidney diseases, such as anti–glomerular basement membrane (GBM) disease, which is characterized by anti–collagen IV (α3NC1) autoantibodies[9] and ANCA vasculitis characterized by antimyeloperoxidase autoantibodies,[10] the antigenic epitopes include both linear peptide sequences and three-dimensional (3D) conformational structure. Knowledge of these antigen epitopes in these conditions has been important for understanding the pathologic disease mechanisms and may help to stratify patient subgroups and disease severity.

PLA2R is a member of the mannose receptor (MR) family, which shares a common domain structure[11] and include the mannose receptor (CD206), Endo180, DEC-205, PLA2R, and FcRY.[12] Detailed structure based on x-ray crystallography for CD206 and conformational studies performed on FcRY have so far been used to predict the structure and function of the domains in PLA2R. However, specific experimental structural data for PLA2R are currently lacking, although this is required to improve the prospect of targeted treatments for patients with IMN.

The interactions between anti-PLA2R and PLA2R are reported to be sensitive to chemical reducing agents, stable in the detergent SDS, and independent of glycosylation. It has been suggested that the pH-dependent extended and bent conformations of the MR family may play a role in exposure of epitopes in PLA2R.[2] It is unlikely that genetically determined amino acid changes in PLA2R specific to cases of IMN could influence immunogenicity or contribute to a 3D conformational disease epitope.[13] One study described linear epitopes within PLA2R using an overlapping array of short peptide sequences derived from PLA2R.[14] Seven linear peptides were tested using ELISA, but no difference was seen between IMN-seropositive patients and control sera. This suggests that 3D conformational structure as described by Beck *et al.*[2] is a critical feature of PLA2R epitopes.

Our strategy was to identify which variably sized constructs of PLA2R react with anti-PLA2R under denaturing conditions (Western blotting) and under nondenaturing conditions (native blotting). We used trypsin digestion of the smallest domain of extracellular PLA2R recognized in Western blotting (N-C3) by anti-PLA2R antibodies and analyzed the immunoreactive fragments by mass spectrometry–based proteomics to determine the constituent peptides. Using experimental data from electron microscopy, we generated a new multidomain model of PLA2R to understand the interaction of anti-PLA2R with PLA2R. We measured the affinity and subclass composition of different anti-PLA2R antibodies. Finally, we confirmed the identity of a major PLA2R epitope by using synthesized candidate peptides to inhibit the binding of autoantibodies to PLA2R as measured by surface plasmon resonance (SPR).

RESULTS

Identification of the Smallest Fragment of PLA2R Reacting by Western Blotting

We generated a series of recombinant PLA2R protein fragments, including full-length extracellular PLA2R (N-C8), the N-terminus to C-type lectin domain (CTLD) 3 (N-C3), the N-terminus to CTLD2 (N-C2), and an isolated ricin domain (Figure 1A). Using Western blotting from SDS-PAGE gels, we compared the reactivity of rabbit anti-PLA2R (characterized in Supplemental Figure 1) and human anti-PLA2R autoantibodies (a pool of 5 sera) against these PLA2R fragments. We found that all of the recombinant fragments were recognized by the rabbit antibody under nondenaturing conditions and in the presence of reducing agent (Figure 1B). By contrast, the human anti-PLA2R recognized all fragments in nondenaturing conditions in the absence of reducing agent but only N-C8 and N-C3 in the presence of reducing agent. Reactivity of the N-C2 fragment and the ricin domain was significantly ablated or abolished, respectively, by reduction in nondenaturing conditions (Figure 1B). We show clearly in the Western blot under denaturing conditions that autoantibodies recognize only N-C8 and N-C3 and that SDS alone destroys the epitope structure in N-C2 and ricin fragments. Finally, to confirm the location of this major epitope to the N-terminal region, we determined the ability of N-C3 to inhibit autoantibody binding using an inhibition ELISA; we found the N-C3 fragment competed effectively for the binding of autoantibodies to N-C8 in approximately 90% of the patient sera tested, confirming the presence of a major epitope within the N-C3 fragment of the receptor (Supplemental Figure 2).

Comparison of the Binding Affinity of Autoantibodies to PLA2R Fragments

We tested sera from four anti-PLA2R–positive patients and showed that the autoantibodies targeted the same conformational epitope as seen on the Western blots of trypsin-fragmented N-C3 (Figure 2A, Supplemental Figure 3). We next determined the affinity of interaction between purified human anti-PLA2R (Supplemental Figure 4) and the four PLA2R constructs (N-C8, N-C3, N-C2, and ricin). The autoantibodies bound with equally strong affinity of approximately 0.1 nM to N-C8, N-C3, N-C2, and the ricin domain, confirming the existence of a single epitope in the protein (Figure 2B). The kinetic constants derived from the analysis of purified antibodies were similar to those obtained from the patient sera, demonstrating the utility of unpurified antibodies in sera and their potential use in a diagnostic assay (Table 1). Moreover, the antibody affinity was similar in all patient sera (all predominantly IgG4) tested at approximately 0.5×10^{-10} M (Supplemental Figure 5, Table 1) and higher than the dissociation constant described for α3NC1 antibodies in anti-GBM disease (2×10^{-9} M).[9]

Effect of pH on PLA2R Conformation and Epitope Availability

PLA2R shares structural similarities with other members of the MR family,[11] and one member, FcRY, undergoes conformational change in a pH-dependent manner.[12] We measured the associated conformational change by monitoring the thickness of the N-C8 protein layer in real time using dual polarization interferometry and determined a susceptible pH

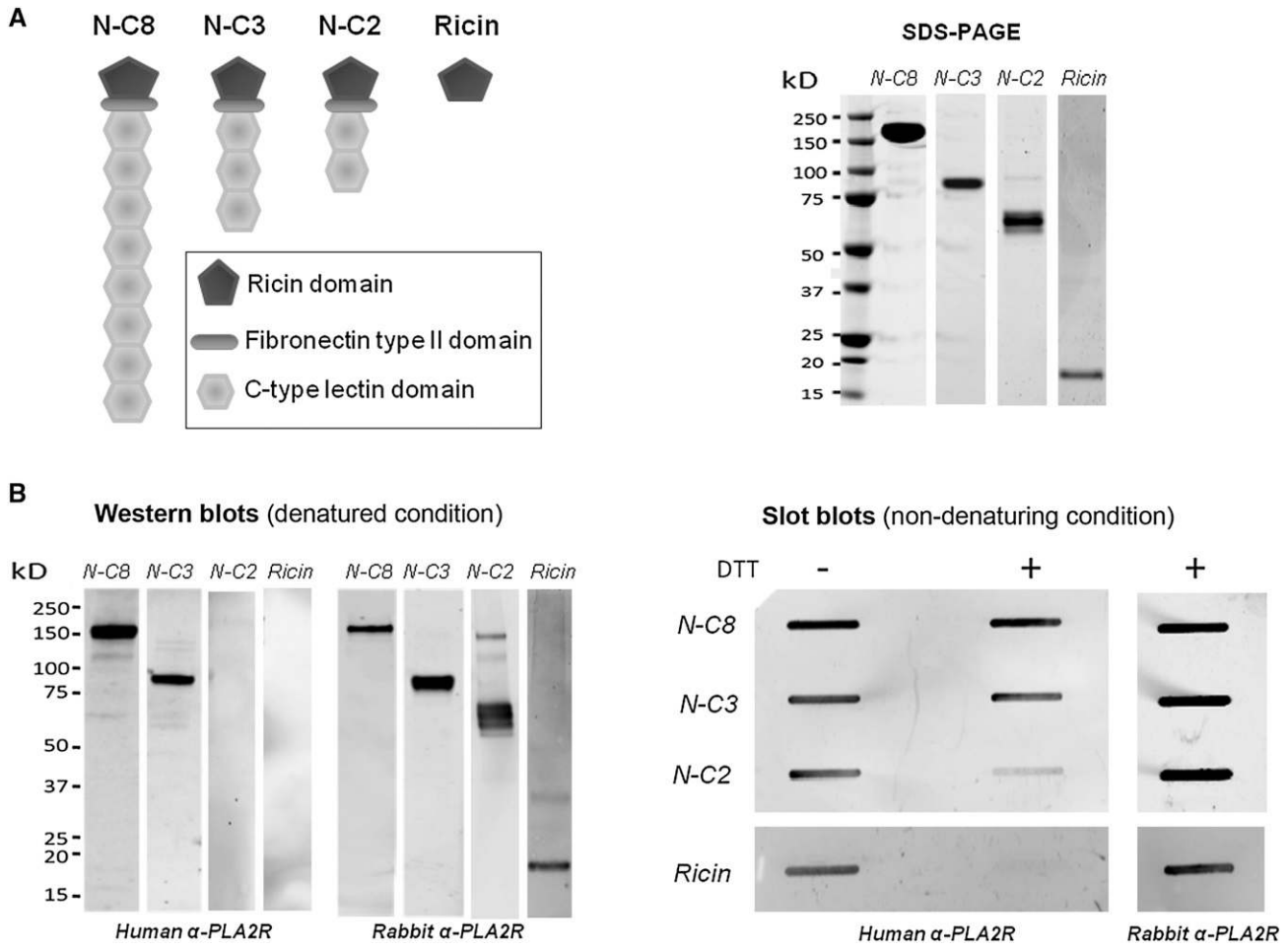

Figure 1. Epitope recognition in PLA2R fragments is dependent on denaturing/non-denaturing conditions. (A) Representations of the extracellular subdomains of a long-fragment PLA2R (N-C8) comprising the N-terminal ricin domain (or cysteine-rich domain), fibronectin type II domain, and 8 C-type lectin domains (CTLD), two shorter fragments ending after the first 3 C-type lectin domains (N-C3) and the first 2 CTLD (N-C2) and the ricin domain. Silver-stained SDS-PAGE gel of purified recombinant N-C8, N-C3, N-C2, and ricin proteins under nonreducing conditions; lane 1 is a molecular mass marker, and subsequent lanes show 1 μg of purified recombinant N-C8 (180 kD), N-C3 (90 kD), N-C2 (65 kD), and ricin (18 kD) proteins. (B) Western blotting analysis of denatured N-C8, N-C3, N-C2, and ricin proteins under nonreduced conditions using a pool of five human sera and rabbit antibodies to PLA2R. Slot blotting analysis of nondenatured N-C8, N-C3, N-C2, and ricin fragments under nonreduced and reduced conditions.

region around pH 6.2 where the transition in conformation occurred (Figure 3A). Both N-C3 and N-C8 variants were then incubated in neutral pH (7.2) and a more acidic pH (6.2), and their sedimentation rates, which depend on the shape and size of the protein, were monitored using analytical ultracentrifugation. At a pH of 7.2, N-C8 sedimented as a single species with a sedimentation coefficient of 8.1s (Figure 3B, Table 2). At a pH of 6.2, the protein became more compact, which was reflected in a larger sedimentation coefficient of 9.2s. The N-C3 data (Figure 3B inset) collected at a pH of 6.2 and of 7.2 yielded an identical sedimentation coefficient (5.3s), indicating that compaction of the molecule at lower pH was specific to the N-C8 receptor and not to the shorter fragment N-C3. To test whether anti-PLA2R binding to N-C8 was independent of this conformational change, single cycle kinetics between the anti-PLA2R antibody and the N-C8 receptor were performed at two pHs (pH of 6.2, tight conformation; pH of 7.2, extended conformation) and showed no difference in affinity (Figure 3C). This indicates that the binding of the autoantibody was not affected by altered conformation of the receptor due to the environmental pH.

Defining a Major Epitope in PLA2R

To locate this major epitope, we generated immunoreactive trypsin fragments of PLA2R under nonreducing conditions. Comparing trypsin-digested and intact PLA2R, we confirmed using the five sera (Table 1) that the epitope reactivity was preserved in the digested antigen (mean$\pm$SEM, 44.8%$\pm$4.2%), data not shown. Trypsin fragmentation of the N-C3 antigen, followed by multidimensional separations (OFFGEL fractionation and

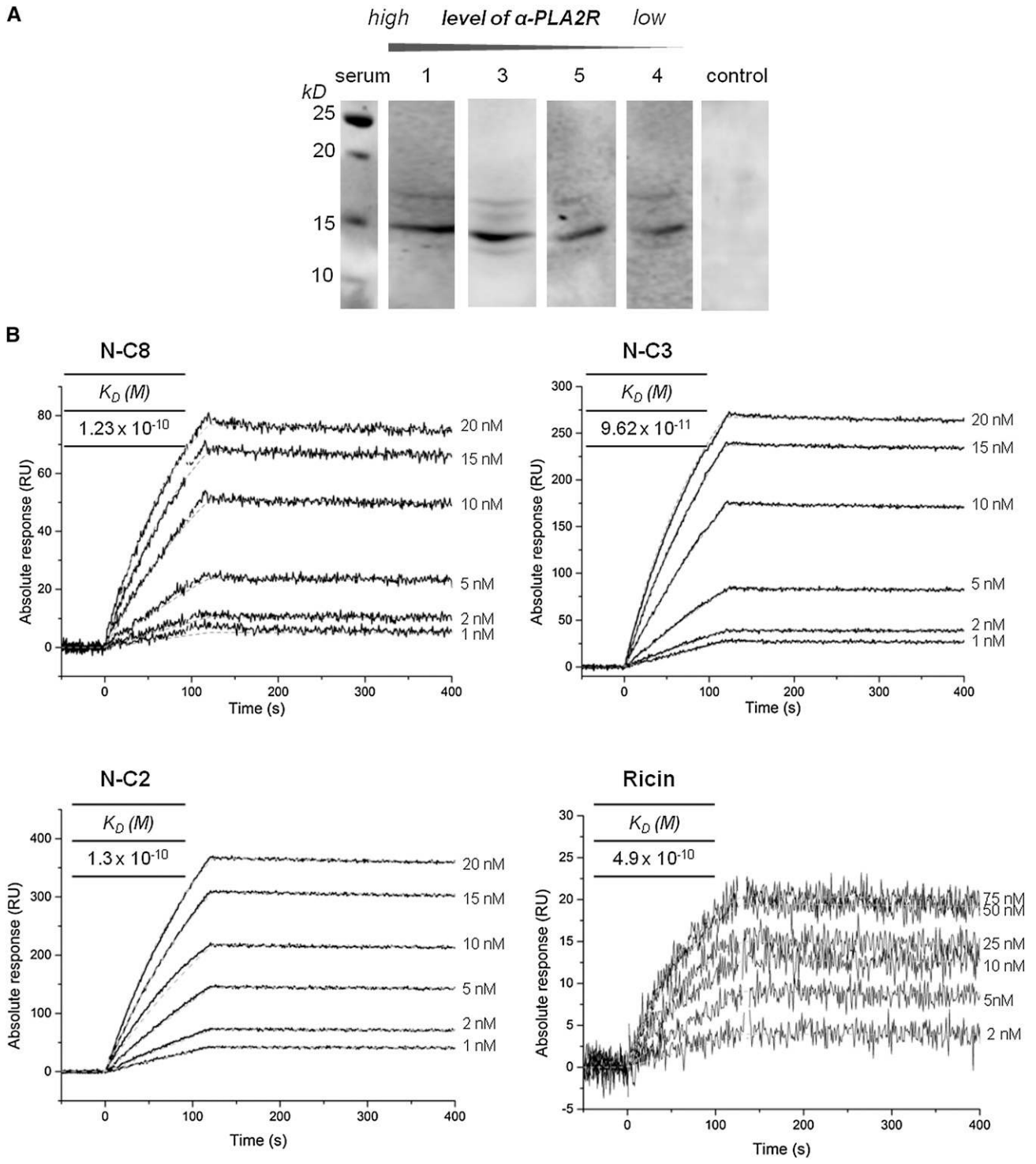

Figure 2. Human anti-PLA2R shows similar binding affinity to N-C8, N-C3, N-C2 and the ricin domain. (A) Western blot analysis of fragmented N-C3 peptides by OFFGEL fractionation using different patient sera. (B) Representative sensorgrams derived from injections of different concentrations of affinity purified anti-PLA2R antibodies over immobilized N-C8 (left panel), N-C3 (right panel), and N-C2 and ricin domain (bottom panels). The tables summarize the kinetic constants of four separate runs for the binding of purified human PLA2R-specific antibody to the PLA2R fragments. Results were obtained after reference subtraction. Kinetics data were fitted to a Langmuir 1:1 interaction model. The association (k_a), dissociation (k_d), and equilibrium (K_D) constants for each run were similar and revealed an overall high binding affinity with an apparent K_D of approximately 0.1 nM.

Table 1. Concentrations, affinity, and IgG subclasses of antibodies to PLA2R

Patients	ELISA (U/ml)	Concentration (μM)	K_D (M)	IgG1 (%)	IgG2 (%)	IgG3 (%)	IgG4 (%)
1	30,000	1.4±0.06	0.49×10^{-10}	16	9	2	72
2	2600	0.32±0.1	0.45×10^{-10}	4	51	0	45
3	30,000	1.0±0.12	0.43×10^{-10}	10	27	0	63
4	2300	0.36±0.19	0.85×10^{-10}	11	10	0	78
5	9300	0.51±0.18	0.32×10^{-10}	17	22	19	42

Absolute concentrations of PLA2R-specific antibody detected in five patient sera tested by ELISA (U/ml) and derived from three kinetic runs (μM). The K_D column is the kinetic constants for the binding of patient autoantibodies to immobilized N-C3. The last four columns indicate the percentage of each IgG subclass (IgG1–4) in the five patient sera measured by ELISA,[5] demonstrating the presence of predominantly IgG4. Values expressed with a plus/minus sign are the mean±SD.

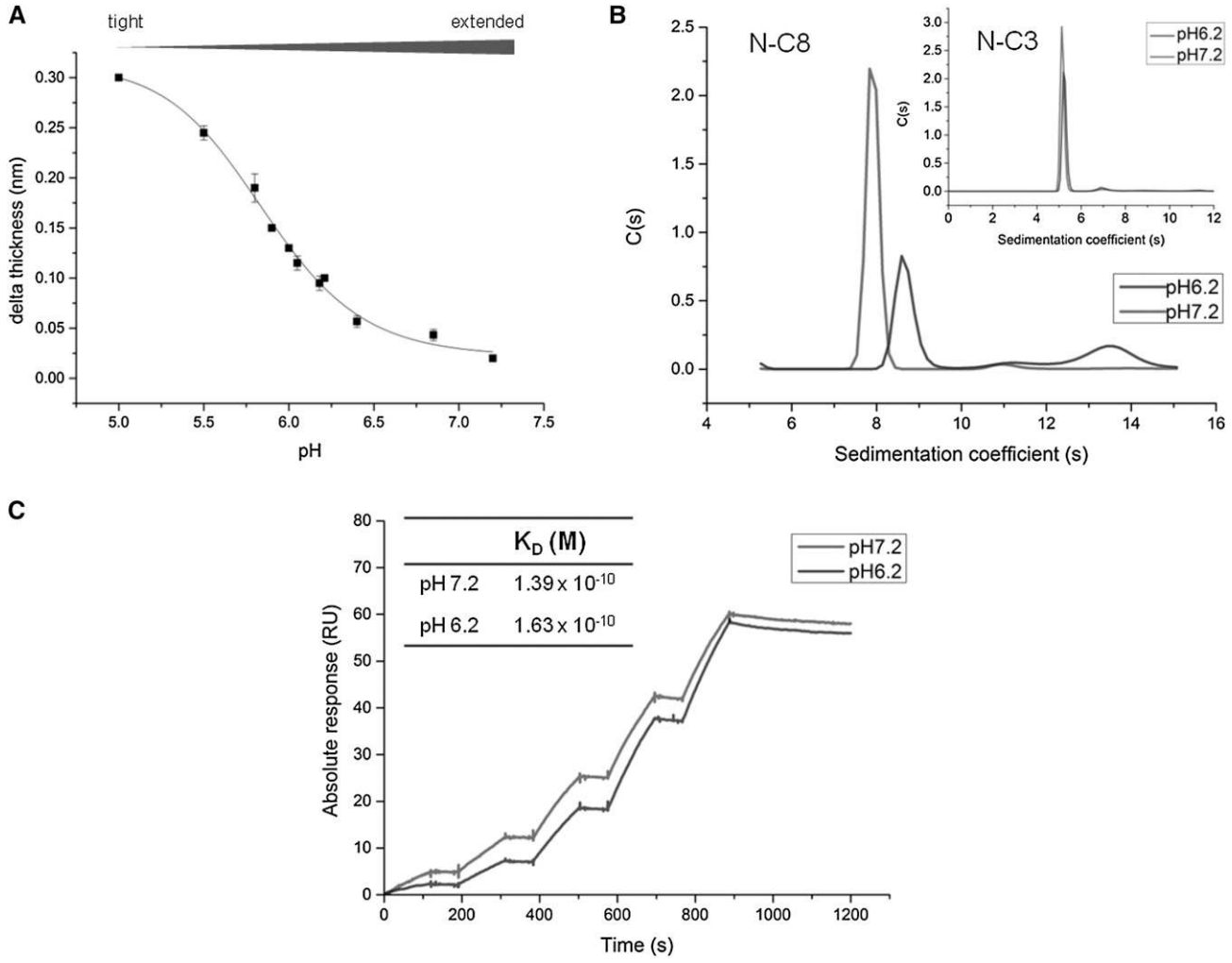

Figure 3. Human anti-PLA2R binding to N-C8 is unaffected by a pH induced conformational change. (A) pH-dependent conformational change of N-C8 determined by dual polarization interferometry. Changes in the thickness of the N-C8 layer as a function of decreasing pH was measured and represented the adsorption behavior of different folded states. (B) Sedimentation velocity of N-C8 and N-C3 (inset) at a pH of 6.2 (black line) and of 7.2 (gray line) analyzed by the distribution of Lamn equation solutions c(s) model using the program Sedfit. (C) Single-cycle kinetics between immobilized purified human PLA2R-specific antibody and N-C8 at a pH of 6.2 and of 7.2. A range of 1, 2, 5, 10, and 15 nM of N-C8 was injected, one cycle at a pH of 6.2 and the other at a pH of 7.2. The surface was not regenerated between injections in each cycle.

SDS-PAGE analysis), were performed to identify the smallest reactive polypeptides in the epitope (Supplemental Figure 3). The polypeptides of interest identified by blotting with anti-PLA2R antibody from patient sera were cut from the gel, reduced and identified by mass spectrometry (MS). MS analysis revealed eight peptides potentially constituting part of the PLA2R epitope (Table 3) and these originated from the ricin domain, FNII domain, CTLD3 domain, and interdomain loops between CTLD 1/2 and CTLD 2/3. The distribution of these peptides is discontinuous on the linear sequence but could be in proximity within

Table 2. Hydrodynamic parameters determined for N-C8 and N-C3 at a pH of 7.4 and a pH of 6.2

Variable	Theoretical Mass (D)	Mass MALLS (D)[a]	Sedimentation Coefficient ($S_{20,w}$)	Frictional Ratio (f/f_0)[b]	Hydrodynamic Radius (nm)[c]
N-C3 (pH 7.4)	79,461	88,820	5.29±0.09	1.38	3.81±0.23
N-C3 (pH 6.2)	79,461	ND	5.35±0.10	1.39	ND
N-C8 (pH 7.4)	164,308	188,800	8.08±0.21	1.51	6.25±0.19
N-C8 (pH 6.2)	164,308	ND	9.23±0.25	1.32	ND

Density, 1.0045 g/ml. Viscosity, 0.01017 poise .*Vbar*, 0.726 for N-C3 and 0.727 for N-C8. ND, not determined.
[a]Calculated with a *dn/dc* of 0.18 ml/g.
[b]f/f_0 from mass derived from MALLS, multi angle light scattering.
[c]Hydrodynamic radius from quasi-elastic light scattering.

the folded molecule and held together by intact disulfide bonds. These eight peptides were synthesized, and we incubated the autoantibody with an excess of the candidate peptides and assessed their potential to inhibit the binding between the autoantibody and its receptor using SPR. Of these peptides, only peptide 1 (GIFVIQSESLKKC), representing the β1 strand, and peptide 2 ([W]SVLTLENCK), forming the β3 strand from the ricin domain, showed significant reduction in binding of purified autoantibody to N-C3 (Figure 4A). By extending peptide 1 toward peptide 2, it also encompasses the β2 strand to form the 31-mer (WQDKGIFVIQSESLKKCIQAGKSVLTLENCK), creating one of the three-dimensional lobes in the β-trefoil structure. This β1,2,3 lobe is also maintained by a disulfide bond connecting the β2 and β3 strands (Figure 5A).[11] The two main competing peptides, peptide 2 and the 31-mer peptide, were titrated in a binding experiment to compete with binding of anti-PLA2R antibody to immobilized N-C3. Peptide 2 showed reproducible inhibition up to 47% and the 31-mer peptide inhibited by 85% (Figure 4B). The competing 31-mer peptide bound to the antibody (with an affinity of approximately 5×10^{-10} M) (Figure 4C), and this resulted in reduced affinity between autoantibody and both N-C3 and N-C2 (Figure 5B) confirming the specificity of the binding.

The rabbit anti-PLA2R antibody did not react with the 31-mer peptide under nondenaturing blotting conditions in contrast to the human anti-PLA2R (pool of 5 sera). Moreover, the reactivity of human anti-PLA2R with the 31-mer peptide was sensitive to reduction (Figure 5A, left panel). The 31-mer peptide in solution is a disulfide-bonded structure illustrated by the shift in the elution profile between the reduced and unreduced state (Figure 5A, right panel). The 3D conformation of the 31-mer peptide identifies the disulfide bond bridging between peptides 1 and 2 (Figure 5A). To identify possible sequence homology for peptides 1 and 2, we used the Basic Local Alignment Search Tool (BLAST)[15] against a database of microbial proteins and found no homology for the peptide 1 sequence. However, the LTLENCK sequence of peptide 2 (SVLTLENCK) was identified in a cell wall enzyme, D-alanyl-D alanine carboxypeptidase, common in several bacterial strains, including *Clostridia* species. This finding may be relevant for pathogenesis of IMN.

3D PLA2R Structure and Arrangement of Domains

There is no multidomain model of PLA2R on which to map these peptide sequences. We therefore produced a 3D structure of the full-length molecule N-C8 using transmission electron microscopy and single particle averaging. We established the relative positioning of the domains and as a result a predicted location of the epitope. Negative stained data were used to visualize the shape of PLA2R (Figure 6A), anti-PLA2R (Supplemental Figure 4) and the preformed isolated immune complex between PLA2R and the autoantibody. Analysis of these datasets allowed us to generate the first 3D structure to a moderate resolution of 20 Angstroms (Supplemental Figure 6) of the extracellular domains of PLA2R (Figure 6B). PLA2R is a flat structure (approximately 4 nm wide) with an overall shape similar to the π symbol, measuring about 12 nm×9 nm. Using homology models of the individual domains, we constructed a structural representation of the domain arrangement informed by the sharp molecular envelope produced from

Table 3. Potential peptides involved in the antibody binding site

Peptide ID	Sequences of Identified Peptides (Residue Numbers)	Sequence Coverage
1	GIFVIQSESLKKC (39–51)	Ricin domain
2	SVLTLENCK (57–65)	Ricin domain
3	EDDLLWCATTSR (198–209)	Fibronectin type II domain
4	YLNHIDHEIVEKDAWK (357–372)	Linker between CTLD1 and CTLD2
5	YYATHCEPGWNPYNR (373–387)	Linker between CTLD1 and CTLD2
6	TWHEALR (399–405)	CTLD2
7	AGHVLSDAESGCQEGWER (504–521)	Linker between CTLD2 and CTLD3
8	YSGGCVAMRGR (613–623)	CTLD3

List generated from the MS analysis of the potential peptides involved in the antibody binding site. Sequences of the identified peptides, the residue numbers as well as their coverage are described in the table.

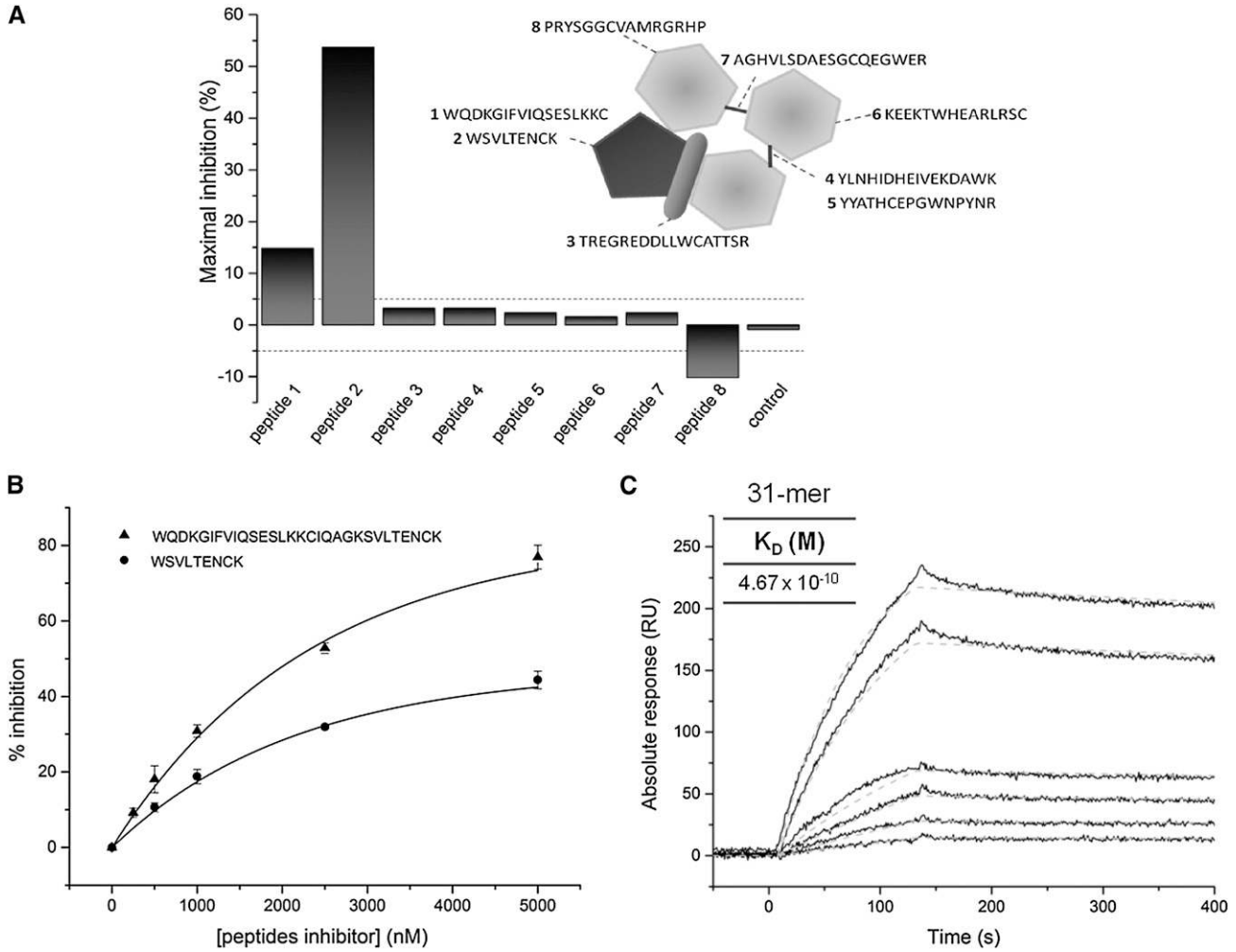

Figure 4. The epitope in the cysteine rich ricin domain is composed of a 31-mer peptide. (A) Screening of inhibitory peptides identified by MS. Sequences of the synthesized peptides as well as their coverage is shown on the schematic diagram of the PLA2R N-C3 fragment. Nine peptides including a control were checked for their inhibitory activity against N-C3. Purified human PLA2R-specific antibody was incubated separately with an excess of each peptide (5 μM) then injected onto the immobilized N-C3. (B) Dose-response curves of inhibition between purified human anti-PLA2R and N-C3 by an increasing amount of peptide 2 and 31-mer peptide. Error bars indicate SDs. (C) Sensorgrams derived from injections of different concentrations of affinity purified PLA2R-specific antibody over captured 31-mer peptide. Kinetics data were fitted to a Langmuir 1:1 interaction model with mass transfer.

transmission electron microscopy (Figure 6B). The resulting models for both N-C3 and N-C8 were analyzed for their hydrodynamic solution properties using the program Hydropro (version 10).[16] The sedimentation coefficients of the models were in good agreement with the compact form of N-C8 and the N-C3 experimental results (Table 2), giving confidence in the overall shape of the molecule. Furthermore, a low-resolution 3D model of the immune complex confirmed the location of the anti-PLA2R binding site in the ricin domain (Supplemental Figure 7).

DISCUSSION

We describe the location and composition of a dominant epitope in PLA2R that interacts with human autoantibodies. Located in the N-terminal CysR ricin domain, the β2-β3 strands of the trefoil structure involve the peptide WQDKGIFVIQSESLKKCIQAGKSVLTLENCK, which forms the focus of this epitope. The crystal structure of this CysR domain is reported as a β-trefoil form also seen in ricin B[17] and is composed of 12 antiparallel β strands: 4 in each part of the 3-lobed -structure. Three disulfide bonds hold these lobes in place, highlighting the structural importance of the disulfide bond present in the 31-mer peptide connecting β2 and β3 strands. Our data show that this epitope in the PLA2R fragments (N-C8, N-C3, N-C2, and ricin domains) in nondenaturing conditions is available to react with human anti-PLA2R autoantibodies. Importantly, the epitope structure is resistant to reduction in the larger species N-C8 and N-C3 but is sensitive to reduction in N-C2, ricin, and the 31-mer peptide. In the SDS-denatured conformations, the

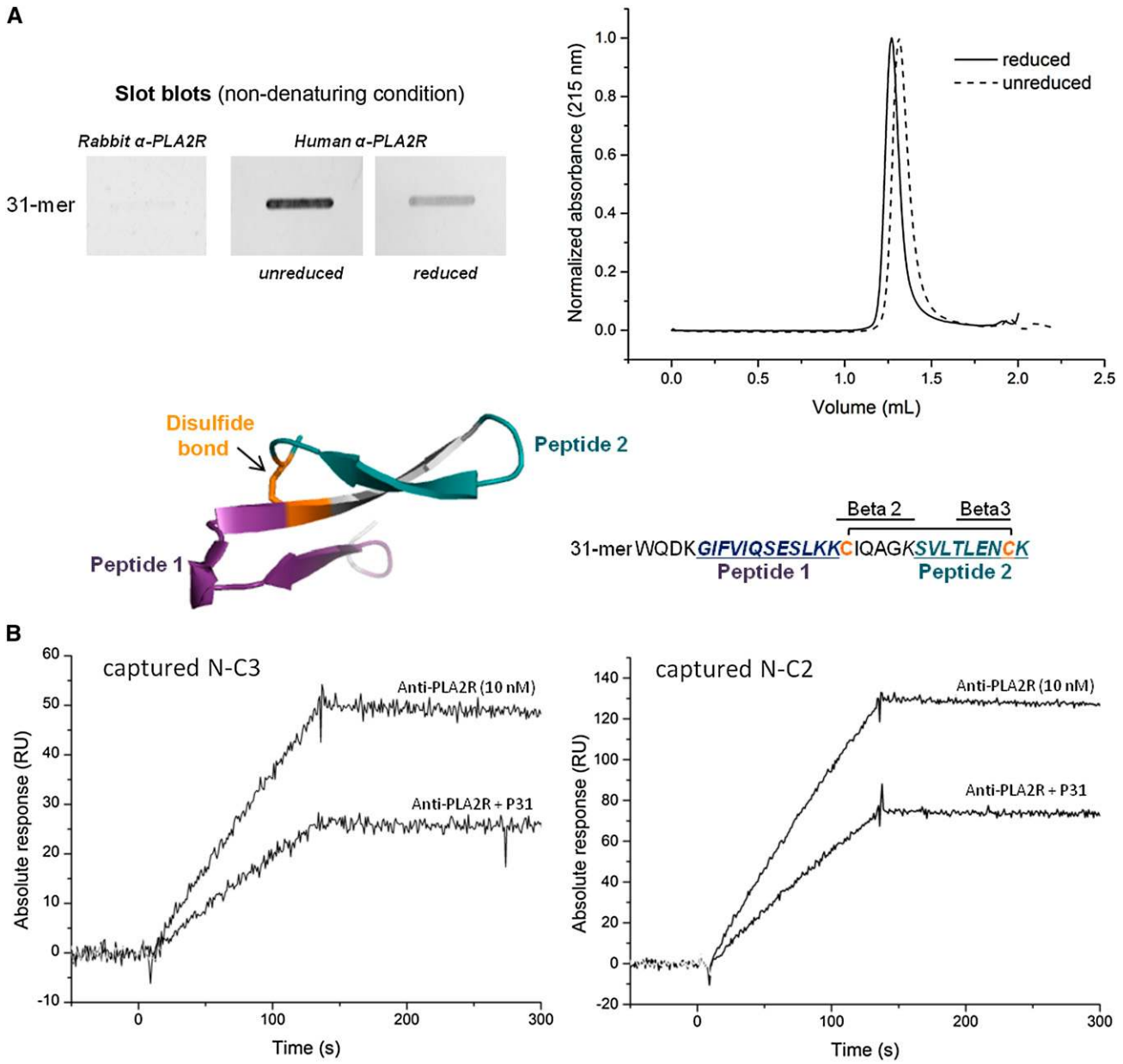

Figure 5. Characterization of the binding pocket. (A) Slot blots analysis of the 31-mer peptide demonstrating the reduction in binding to the autoantibody under reducing conditions. 3D cartoon representation of the 31-mer peptide structure comprising peptide 1 and peptide 2 (dark gray) with the disulfide bond bridging the two peptides. Inset: gel filtration elution profiles of the nonreduced and reduced 31-mer peptide showing its cyclic nature in native form. (B) SPR inhibition analysis of the binding between the human autoantibody and captured N-C3 (left) or N-C2 (right) by the human 31-mer peptide.

epitope is preserved only in N-C8 and N-C3 but not N-C2 and ricin. This clearly shows that the larger fragments N-C8 and N-C3 possess additional conformational interdomain properties that protect the epitope from SDS denaturation or reduction. However, as described by Beck *et al.*, the combination of SDS denaturation and reduction destroys the epitope in the N-C8 extracellular sequence (Supplemental Figure 8).

Our current best-fit model of the preformed immune complex of PLA2R and anti-PLA2R confirms that the IgG Fab binds to PLA2R in the area of the ricin/CTLD3 interaction. Current knowledge of the PLA2R sequence derived from gene sequencing suggests that the PLA2R protein structure in patients with IMN is not significantly different from that of healthy controls.[13] Other potential mechanisms affecting antigen conformation and aberrant immune processing need exploring to understand how PLA2R becomes immunogenic. We described a pH-dependent conformational change in PLA2R (N-C8), as previously reported for FcRY,[12] and show

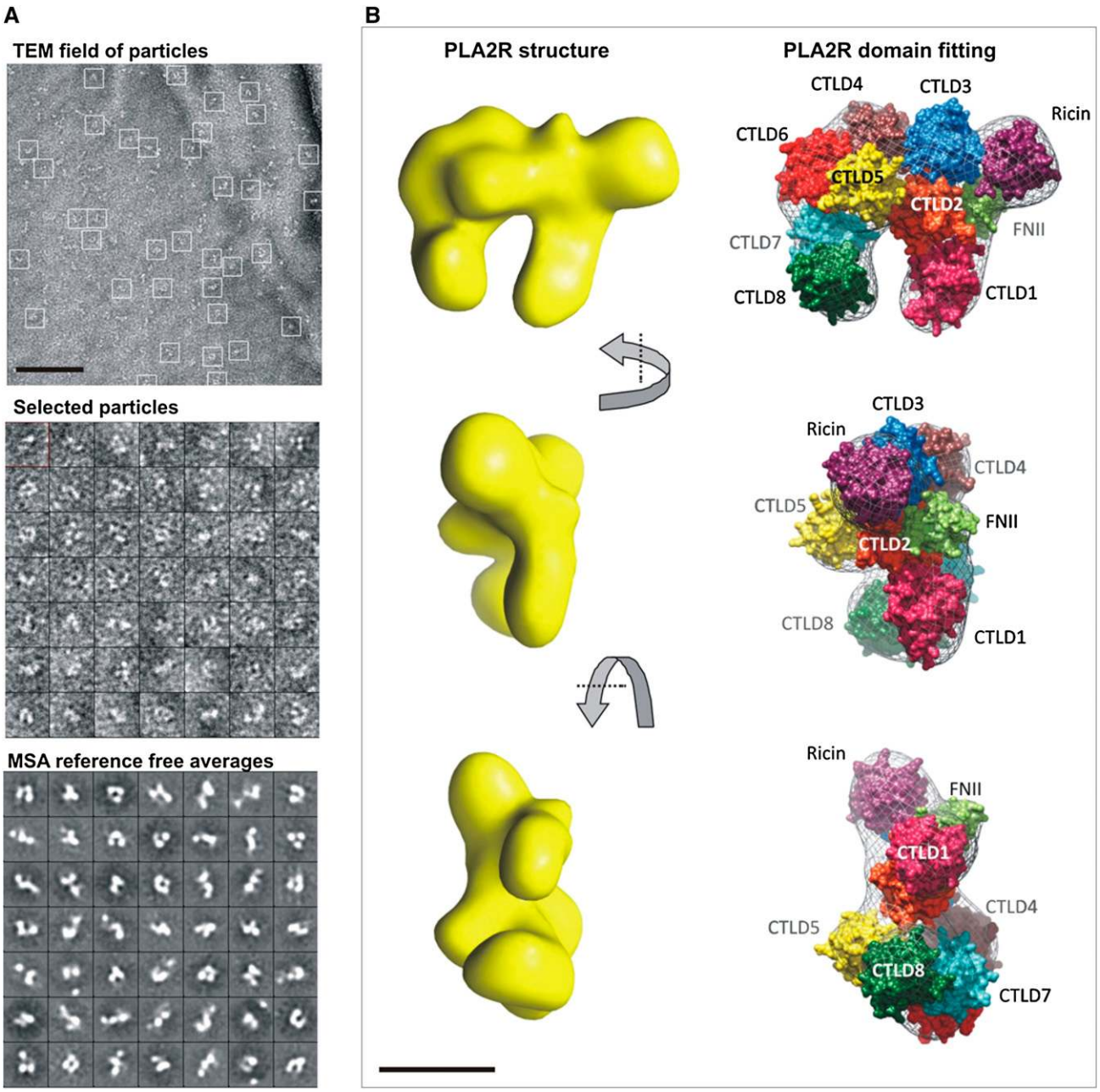

Figure 6. 3D PLA2R model structure and arrangement of domains. (A) Representative area micrographs of N-C8 with highlighted images of single molecules within white squares, selected projections obtained and two-dimensional averages of the images within the corresponding class. Scale bar=1000 Å. TEM, transmission electron microscopy; MSA, multi statistical analysis. (B) Electron density of N-C8 solved from approximately 20,000 selected particles at 20-Å resolution and a 3D reconstruction of N-C8 showing the domains arrangement. Individual PLA2R domains were modeled using Phyre2. The domains were aligned in the electron microscopic density map using Chimera and validated using area under the curve hydrodynamics parameters (Table 2). Scale bar=50 Å.

that this is not a property of the N-C3 fragment and does not influence the affinity of antibody interaction. This eliminates conformation change due to pH<6.2, which can be present in inflammatory tissue abnormalities and in subcellular compartments of leukocytes as a major contributor to immunogenicity. However, our evidence-based model describes the adjacency of the ricin and CTLD3 domains in a ring-like configuration, unlike the linear sequence commonly illustrated in cartoons. This 3D conformational structure may be important for stability of the epitope in N-C3 and may explain its resistance to denaturation (SDS) or reduction, to which N-C2 lacking CTLD3 is susceptible. Our current structural model requires further confirmation from x-ray crystallography studies.

Potentially, the stability of the epitope in soluble forms of PLA2R under physiologic conditions may facilitate selection of B cells for generation of class II peptides to present to T cells. This is a testable hypothesis for immunogenicity and is a significant step toward understanding the initiation of the autoimmune mechanism in IMN. Interestingly, approximately 10% of anti-PLA2R positive sera react variably to another epitope that is not in N-C3 fragment and that by implication is in C4-C8 region of PLA2R. Further work is needed to identify the nature of this second epitope and whether antibodies to this minor epitope are associated with a particular clinical phenotype of IMN.

The affinity of anti-PLA2R antibodies in different patient sera is uniformly high and approximately 2- to 5-fold greater than that described for the classic autoantibody anti–collagen IV (α3NC1).[9] This could explain the clinical paradox of PLA2R-positive biopsy specimens associated with absence of anti-PLA2R antibodies in the serum.[18,19] We suggest that as anti-PLA2R antibodies are secreted by plasma cells, the high affinity of the antibody will ensure the autoantibody is adsorbed out of serum onto PLA2R positive cells, such as podocytes, until the rate of production of antibody exceeds the rate of removal from the serum; at this point there will be free detectable circulating anti-PLA2R. These biopsy-positive, seronegative cases may, therefore, represent an early phase of the immunologic abnormality seen in primary disease and in recurrent disease after transplantation.[20]

Having identified the β2-β3 strands (31-mer peptide) containing an inherent disulfide bond, we mapped this peptide to the reported ricin domain structure. It will be important to further investigate how the availability of this binding pocket to autoantibodies is controlled by adjacent domains. It has been proposed that the induction of autoimmunity may be mechanistically driven by infection, whereby an immune response against bacterial or viral agent cross-reacts with a self-component. In this regard, preliminary bioinformatic analysis of peptide 2 in BLAST searches against microbial protein databases revealed complete homology for the sequence LTLENCK, which is part of the bacterial cell wall enzyme D-alanyl-D alanine carboxypeptidase common to *Clostridium* species and other bacteria. Clonal expansion of B cells driven by common infections may allow MN genetically susceptible individuals to bind PLA2R through the B cell receptor, ingest, degrade, and present PLA2R peptides on class II receptors (coded by pathologic alleles of DQA1) to engage T cell help and promote autoantibody production. In autoimmune mechanisms over time, there is often a change in use of epitopes on the autoantigen, in some cases as proposed for anti-GBM antibodies, the binding of the autoantibody induces neo-epitopes initiating "epitope spreading."[9] Now that we have defined a major epitope, we can investigate whether use of this epitope changes over time in chronic MN disease, from initiation and first presentation of disease through induction of remission, relapse, and recurrent disease after transplantation.

Knowledge of this PLA2R epitope is potentially useful in developing novel therapies for translation into the clinic for patient benefit. The use of the 31-mer peptide as an inhibitor of anti-PLA2R binding to the podocyte may modulate the consequences of anti-PLA2R–mediated cell biology. Alternatively, the 31-mer peptide coupled to immunoadsorption columns could provide an effective means of specifically removing anti-PLA2R in conjunction with immunosuppression, particularly for patients resistant to standard mainline immunosuppressive drugs.

CONCISE METHODS

Cloning, Expression, and Purification of PLA2R N-C8, N-C3, and N-C2 and the Ricin Domain

The previously described[5] codon-optimized clone of human extracellular PLA2R (N-C8) was modified to generate the smaller PLA2R fragments expression vectors (details in Supplemental Methods). The resulting constructs were transfected into HEK293-EBNA1 cells (human embryonic kidney cells; Invitrogen) using Lipofectamine 2000 reagent (Invitrogen). The secreted proteins were purified using nickel affinity chromatography. Conditioned medium containing 20 mM imidazole was loaded onto a 5-ml HiTrap Excell nickel affinity chromatography column (GE Healthcare). Bound proteins were eluted by using a linear gradient of 20–500 mM imidazole over 10 column volumes in a buffer containing 10 mM BisTris and 150 mM NaCl (pH, 7.2). The PLA2R-containing fractions were desalted using PD-10 columns (GE Healthcare) into 10 mM BisTris (pH, 7.2) and further purified by anion exchange chromatography on a MiniQ column using the Ettan purifier HPLC system (GE Healthcare). The proteins were eluted by using a linear gradient of 0–1 M NaCl. Buffer conditions were optimized using an Optim screening instrument (Avacta).

N-C3 Inhibition ELISA

The ELISA method was a variation on the standard assay previously described.[5] Briefly, PLA2R (N-C8) at 125 ng/ml was coated onto ELISA plates overnight and plates blocked with Superblock (Thermo Fisher Scientific). Fifty microliters of 1:100 dilution of patient serum plus 50 μl of buffer or NC-3 fragment (to give a final concentration in the well of 9.0 μg/ml, 0.9 μg/ml, 0.09 μg/ml, and 0.009 μg/ml) were preincubated for 2 hours at room temperature before adding to the ELISA plate for a further 2 hours with shaking. Following extensive washing, antihuman IgG-horseradish peroxidase at 1:25,000 dilution in assay buffer was added to all wells for 2-hour incubation. Following washing, the plate was developed by adding substrate, and the reaction terminated at 5 minutes by addition of 1 M H_2SO_4. Plates were read at 450 nm and inhibition curves constructed. The concentration of 9.0 μg/ml was used to compare the inhibition profile of 43 different sera previously reported as anti-PLA2R positive. This experiment could be repeated with just the ricin domain to confirm that there are no adjacent epitopes in FN II or CTLD1–3.

Binding Studies Using SPR

Purified recombinant N-C8, N-C3, N-C2, and ricin proteins (50–100 μg/ml) diluted in 10 mM sodium acetate at a pH of 4.5 were immobilized on a ProteOn GLM sensor chip using standard amine coupling

chemistry. Ligand densities of 6000 RU, 5000 RU, 5000 RU, and 500 RU, respectively, were achieved. The first set of kinetic runs were performed using 6 concentrations of purified anti-PLA2R antibody as analytes (1, 2, 5, 10, 15, and 20 nM) in HEPES buffer (pH, 7.2) containing 0.005% Tween 20. Each injection lasted 120 seconds at a flow rate of 80 μl/ml with a 900-second dissociation phase. Tightly bound proteins were then dissociated by two successive (40 seconds) injections of 100 mM glycine (pH, 2.2). The second series of kinetic used patient sera. Seven dilutions of sera containing anti-PLA2R antibody (1/100, 1/200, 1/500, 1/800, 1/1000, 1/1500, and 1/2000) were injected onto the same immobilized N-C8 and N-C3 proteins. Samples were all double-referenced with blank row (injected with running buffer) and control serum. The data were analyzed and fitted to a Langmuir 1:1 interaction model. Single cycle kinetics between immobilized purified anti-PLA2R antibody (2000 RU bound onto a CM5 sensor chip) and N-C8 were performed on a BIAcore T200 instrument (BIAcore AB). Two cycles of 1, 2, 5, 10, and 15 nM of N-C8 were injected, one at a pH of 6.2 and the other at a pH of 7.2. Kinetic parameters were determined with the manufacturer's BIAevaluation 4.1 software. Peptide inhibition assays were carried out as follows. Each individual peptide (5 μM) was incubated with 10 nM of human purified anti-PLA2R antibody for 1 hour; then the complex was injected on the captured N-C3 (5000 RU bound). Peptides 2 and 31-mer peptide were titrated to compete the binding between anti-PLA2R antibody and N-C3 with a range of 0-, 0.25-, 0.75-, 1-, 2-, 3-, and 5-μM peptides.

Determination of Anti-PLA2R Antibody Concentration in Patient Sera

Quantitation of serum antibody concentrations was performed on the Proteon XPR-36 (Bio-Rad) SPR instrument, where the initial binding rates of purified human anti-PLA2R binding to N-C3 were used as standard curve to determine the concentration of anti-PLA2R in the unknown serum samples.

Dual Polarization Interferometry

Dual polarization interferometry was used to provide quantitative information on the thickness, the refractive index and density of the immobilized PLA2R layer with the capability to measure conformational change in real time. These experiments were performed on a Farfield AnaLight instrument. Purified recombinant N-C8 and N-C3 proteins (at a concentration of 50 μg/ml) were immobilized onto an amine functionalized AnaChip using sulfo-GMBS (Pierce) an amine-to-sulfhydryl crosslinker (2 mg/ml). After stabilizing the immobilized N-C8 and N-C3 with sufficient rinsing with BisTris running buffer (10 mM BisTris [pH, 7.2], 150 mM NaCl), the proteins were then exposed to a decreasing pH range (pH, 7.2, 6.8, 6.4, 6.2, 6, 5.9, 5.8, 5.5, and 5). N-C8 and N-C3 were regenerated between the different pHs with running buffer (pH, 7.2). Analysis of the raw data and determination of density, thickness, and mass per unit area were performed using the *Ana*Light Bio200 analysis software (Farfield Scientific).

Structure Analysis by Sedimentation Velocity

The sedimentation coefficients for recombinant N-C8 and N-C3 proteins (at 150 μg/ml) were determined from velocity experiments using the Optima XL-A ultracentrifuge (Beckman Instruments).The experiments were performed using double sector cells and a rotor speed of 74,500 *g* for N-C8 and 116,500 *g* for N-C3, taking 150 scans at 1.5-minute intervals at a wavelength of 280 nm and at a temperature of 20°C. The sedimenting boundaries were analyzed using the program Sedfit, version 8.7.[21]

OFFGEL Fractionation and Mass Spectrometry Analysis

N-C8 and N-C3 purified proteins (300 μg) were digested with 15 μg proteomics grade trypsin (Sigma-Aldrich) overnight at 37°C. Polypeptides (nonreduced) were separated by isoelectric point and size and the smallest fragments were identified by western blotting with patient sera. Bands of interest corresponding to the reactive bands on the Western blot were excised and in-gel tryptic digestion was performed. Dried gel pieces were reduced with 10 mM dithiothreitol and alkylated with 55 mM iodoacetamide. Digested samples were analyzed by liquid chromatography-MS /MS using an UltiMate 3000 Rapid Separation LC (RSLC; Dionex Corporation) coupled to a LTQ Velos Pro (Thermo Fisher Scientific) mass spectrometer. Data produced were searched using Mascot (Matrix Science, London, UK) against the Uniprot_human database, version 2011_05_03. Data were validated using Scaffold (Proteome Software).

Negatively Stained Transmission Electron Microscopy

Negatively stained samples of PLA2R, antibody, or the PLA2R-antibody complex (10–20 μg/ml) were absorbed to the surface of a freshly glow-discharged 400 mesh carbon coated grid (EMS) for 30 seconds, washed twice in 10-μl droplets of distilled water, and then placed on a 10-μl droplet of 5% (wt/vol) uranyl acetate for 30 seconds and air dried. Low-dose data (10–20e-/Å) were recorded on a G30 Polara operating at 200 kV and a nominal magnification of 39,000× with a Gatan 4K CCD camera. CCD images were recorded with a 1-second exposure at defocus values between 0.5 and 2.5 μm and at a sampling increment of 3.05 Å/pixel.

Single-Particle Analysis and 3D structure Determination

Single-particle averaging was performed using EMAN2.[22] Data-sets were selected using a combination of manual and semi-automated swarm picking. Following full CTF correction, each dataset was subjected to multi statistical analysis 2D classification using cross correlation coefficient as the main comparator. A selection of uniquely positioned projection averages were selected and used to generate an initial 3D model for refinement (C1 symmetry was applied to the processing for all datasets). This model was used as a start model for eight rounds of iterative refinement, using FRC as the main alignment comparator, to produce a self-consistent 3D structure that was low-pass-Gaussian filtered to 20-Å resolution. Resolution estimates of the final structures were determined using the Fourier shell correlation with a cutoff value of 0.5. 3D volumes were examined and modeling was performed using Chimera.[23]

Modeling

Homology models of the domains were generated using the software Phyre2.[24] These were assembled into the electron microscopic density map using Chimera, version 1.8, without the interglobular linkers

present. The resulting models of both the N-C3 and N-C8 were converted to shell models using the program Hydropro10.[16] The hydrodynamic outputs were compared with experimental data for the hydrodynamic radius deduced from light scattering, and sedimentation coefficient determined using analytical ultracentrifugation, in order to establish the best arrangement of the domains.

ACKNOWLEDGMENTS

Special thanks go to Marjorie Howard for her help with the protein characterization, David Knight for his advice on mass spectrometry, Michael J. Randles for his help with microscopy, and Catherine Keeling for immunohistochemistry.

This research was supported financially by a Medical Research Council Project grant MR/J010847/1, Kidney Research UK grant RP56/2012, EU Framework 7 Programme Grant 305608, "EURenOmics" and by a Wellcome Trust Institutional Strategic Support Fund (ISSF) award (097820) to the University of Manchester. R.L. was supported by a Wellcome Trust Intermediate Clinical Fellowship (WT0900006). We also acknowledge support from the Manchester Academic Healthcare Science Centre (MAHSC) (186/200). An abstract of this research was presented at the American Society of Nephrology in Atlanta, Georgia, in 2013.

DISCLOSURES

None.

REFERENCES

1. McQuarrie EP, Mackinnon B, Stewart GA, Geddes CC; Scottish Renal Biopsy Registry: Membranous nephropathy remains the commonest primary cause of nephrotic syndrome in a northern European Caucasian population. *Nephrol Dial Transplant* 25: 1009–1010, author reply 1010–1011, 2010
2. Beck LH Jr, Bonegio RG, Lambeau G, Beck DM, Powell DW, Cummins TD, Klein JB, Salant DJ: M-type phospholipase A2 receptor as target antigen in idiopathic membranous nephropathy. *N Engl J Med* 361: 11–21, 2009
3. Stanescu HC, Arcos-Burgos M, Medlar A, Bockenhauer D, Kottgen A, Dragomirescu L, Voinescu C, Patel N, Pearce K, Hubank M, Stephens HA, Laundy V, Padmanabhan S, Zawadzka A, Hofstra JM, Coenen MJ, den Heijer M, Kiemeney LA, Bacq-Daian D, Stengel B, Powis SH, Brenchley P, Feehally J, Rees AJ, Debiec H, Wetzels JF, Ronco P, Mathieson PW, Kleta R: Risk HLA-DQA1 and PLA(2)R1 alleles in idiopathic membranous nephropathy. *N Engl J Med* 364: 616–626, 2011
4. Hofstra JM, Beck LH Jr, Beck DM, Wetzels JF, Salant DJ: Anti-phospholipase A_2 receptor antibodies correlate with clinical status in idiopathic membranous nephropathy. *Clin J Am Soc Nephrol* 6: 1286–1291, 2011
5. Kanigicherla D, Gummadova J, McKenzie EA, Roberts SA, Harris S, Nikam M, Poulton K, McWilliam L, Short CD, Venning M, Brenchley PE: Anti-PLA2R antibodies measured by ELISA predict long-term outcome in a prevalent population of patients with idiopathic membranous nephropathy. *Kidney Int* 83: 940–948, 2013
6. Hoxha E, Thiele I, Zahner G, Panzer U, Harendza S, Stahl RA: Phospholipase A2 receptor autoantibodies and clinical outcome in patients with primary membranous nephropathy. *J Am Soc Nephrol* 25: 1357–1366, 2014
7. Hofstra JM, Debiec H, Short CD, Pellé T, Kleta R, Mathieson PW, Ronco P, Brenchley PE, Wetzels JF: Antiphospholipase A2 receptor antibody titer and subclass in idiopathic membranous nephropathy. *J Am Soc Nephrol* 23: 1735–1743, 2012
8. Bech AP, Hofstra JM, Brenchley PE, Wetzels JF: Association of Anti-PLA2R Antibodies with outcomes after immunosuppressive therapy in idiopathic membranous nephropathy. *Clin J Am Soc Nephrol* 9: 1386–1392, 2014
9. Pedchenko V, Bondar O, Fogo AB, Vanacore R, Voziyan P, Kitching AR, Wieslander J, Kashtan C, Borza DB, Neilson EG, Wilson CB, Hudson BG: Molecular architecture of the Goodpasture autoantigen in anti-GBM nephritis. *N Engl J Med* 363: 343–354, 2010
10. Roth AJ, Ooi JD, Hess JJ, van Timmeren MM, Berg EA, Poulton CE, McGregor J, Burkart M, Hogan SL, Hu Y, Winnik W, Nachman PH, Stegeman CA, Niles J, Heeringa P, Kitching AR, Holdsworth S, Jennette JC, Preston GA, Falk RJ: Epitope specificity determines pathogenicity and detectability in ANCA-associated vasculitis. *J Clin Invest* 123: 1773–1783, 2013
11. East L, Isacke CM: The mannose receptor family. *Biochim Biophys Acta* 1572: 364–386, 2002
12. West AP Jr, Herr AB, Bjorkman PJ: The chicken yolk sac IgY receptor, a functional equivalent of the mammalian MHC-related Fc receptor, is a phospholipase A2 receptor homolog. *Immunity* 20: 601–610, 2004
13. Coenen MJ, Hofstra JM, Debiec H, Stanescu HC, Medlar AJ, Stengel B, Boland-Augé A, Groothuismink JM, Bockenhauer D, Powis SH, Mathieson PW, Brenchley PE, Kleta R, Wetzels JF, Ronco P: Phospholipase A2 receptor (PLA2R1) sequence variants in idiopathic membranous nephropathy. *J Am Soc Nephrol* 24: 677–683, 2013
14. Behnert A, Fritzler MJ, Teng B, Zhang M, Bollig F, Haller H, Skoberne A, Mahler M, Schiffer M: An anti-phospholipase A2 receptor quantitative immunoassay and epitope analysis in membranous nephropathy reveals different antigenic domains of the receptor. *PLoS ONE* 8: e61669, 2013
15. Altschul SF, Madden TL, Schäffer AA, Zhang J, Zhang Z, Miller W, Lipman DJ: Gapped BLAST and PSI-BLAST: A new generation of protein database search programs. *Nucleic Acids Res* 25: 3389–3402, 1997
16. Ortega A, Amorós D, García de la Torre J: Prediction of hydrodynamic and other solution properties of rigid proteins from atomic- and residue-level models. *Biophys J* 101: 892–898, 2011
17. Liu Y, Chirino AJ, Misulovin Z, Leteux C, Feizi T, Nussenzweig MC, Bjorkman PJ: Crystal structure of the cysteine-rich domain of mannose receptor complexed with a sulfated carbohydrate ligand. *J Exp Med* 191: 1105–1116, 2000
18. Debiec H, Ronco P: PLA2R autoantibodies and PLA2R glomerular deposits in membranous nephropathy. *N Engl J Med* 364: 689–690, 2011
19. Svobodova B, Honsova E, Ronco P, Tesar V, Debiec H: Kidney biopsy is a sensitive tool for retrospective diagnosis of PLA2R-related membranous nephropathy. *Nephrol Dial Transplant* 28: 1839–1844, 2013
20. Debiec H, Ronco P: Immunopathogenesis of membranous nephropathy: An update. *Semin Immunopathol* 36: 381–397, 2014
21. Schuck P: Size-distribution analysis of macromolecules by sedimentation velocity ultracentrifugation and lamm equation modeling. *Biophys J* 78: 1606–1619, 2000
22. Tang G, Peng L, Baldwin PR, Mann DS, Jiang W, Rees I, Ludtke SJ: EMAN2: An extensible image processing suite for electron microscopy. *J Struct Biol* 157: 38–46, 2007
23. Pettersen EF, Goddard TD, Huang CC, Couch GS, Greenblatt DM, Meng EC, Ferrin TE: UCSF Chimera—a visualization system for exploratory research and analysis. *J Comput Chem* 25: 1605–1612, 2004
24. Kelley LA, Sternberg MJ: Protein structure prediction on the Web: A case study using the Phyre server. *Nat Protoc* 4: 363–371, 2009

See related editorial, "The Dominant Humoral Epitope in Phospholipase A_2 Receptor-1: Presentation Matters When Serving Up a Slice of π," on pages 237–239.

This article contains supplemental material online at http://jasn.asnjournals.org/lookup/suppl/doi:10.1681/ASN.2014050502/-/DCSupplemental.